교육학석사학위논문

Development and Validation of Prostate Specific Antigen Immunoassay Platform based on Surface Enhanced Raman Spectroscopic Nanoprobe

표면 증강 라만 산란 기반 나노프로브를 이용한 전립선암 면역분석 플랫폼 유효성 검증에 관한 연구

2018 년 8월

서울대학교 대학원

과학교육과 화학전공

조 유 진

Development and Validation of Prostate Specific Antigen Immunoassay Platform based on Surfaced Enhanced Raman Spectroscopic Nanoprobe

지도교수 정 대 홍

이 논문을 교육학 석사 학위논문으로 제출함

2018 년 8 월

서울대학교 대학원

과학교육과 화학전공

조 유 진

조유진의 교육학석사 학위논문을 인준함

2018 년 8 월

위 원 장 _____ (인)

부위원장 _____ (인)

위 원 _____ (인)

Abstract

Development and Validation of Prostate Specific Antigen Immunoassay Platform based on Surfaced Enhanced Raman Spectroscopic Nanoprobe

Yoojin Cho

Department of Science Education

(Major in Chemistry)

The Graduate School

Seoul National University

SERS (Surfaced-enhanced Raman Scattering) based immunoassay have drawn significant attention as the diagnostic tools for the detection of

biochemical targets because of their high sensitivity, lower photobleaching and multiplexing capability. However, some troubles have been existed when diverse SERS-based immunoassay platforms are applied to practical or commercial use due to lack of validation and optimization study about each immunoassay step. In this research, we try to validate and develop a SERS-based immunoassay platform for getting reproducible and reliable assay results using sandwich immunocomplex concept with chip-based platform. Experiments were carried out by three approaches for validating immunoassay platform: (1) synthesis about three different kinds of SERS Dots and characterization with SERS signal for validating uniformity and stability of SERS Dots by single particle detection. (2) validation of nanoprobes: optimization of antibody conjugation technique and evaluating of bioactivity (3) chip substrate validation: optimization of capture antibody onto substrate, evaluating of bioactivity and non-specific binding control test. To confirm our validation approaches, we performed SERS-based immunoassay with prostate specific antigen (PSA) as a target biomarker, and then PSA could be detected high sensitivity (ca. 0.05 pg/mL LOD) with a wide dynamic range (0.0001 – 1 ng/mL). Our validated and developed SERS-based immunoassay platform will be applied to other types of biomarkers detection with any other different platforms for its step-by-step validation data.

Keywords: Surface-enhanced Raman Scattering (SERS), immunoassay, sandwich immunocomplex platform, validation, SERS nanoprobe, Prostate Specific Antigen (PSA), high sensitivity

Student number: 2016-21587

Contents

List of Figures

List of Scheme

1. Introduction

Immunoassay is a biochemical analysis technique for diagnosing cancer or other types of diseases based on specific interactions between antibodies (Abs) and antigens[1-6]. Normally, enzyme-linked immunsorbent assay (ELISA)[7-9], fluorescence[10, 11] and surface plasmon resonance (SPR)[12, 13] and chemiluminescence[14, 15] are being widely used as technical tools for immunoassay. However, these techniques have several drawbacks such as a low signal reproducibility, photobleaching and broad emission bands.

To solve these problems, many scientists have been interested in SERS (Surfaced-enhanced Raman Scattering) based immunoassay technique for its high sensitivity, lower photobleaching and multiplex detection capability[16-19]. SERS is a phenomenon in which the Raman scattering signal is greatly enhanced by the electric field on the metal surface when it is illuminated by an external light source. The enhancement of the Raman signal by metal surfaces allows for detection with high sensitivity. Furthermore, multiple types of biomarkers can be detected simultaneously due to the relative narrow band width of the Raman signal.[20, 21] Based on

these properties, SERS-based immunoassay has a great potential for overcoming the problems inherent in conventional immunoassay.

One of the most universal platforms for SERS-based immunoassay is the detection of a sandwich immunocomplex immobilized on supporting substrate such as chips[22-24], microfluidic chips[25-27], lateral flow assay (LFA) strips[28-30] and magnetic beads[31-33] using antibody or DNA-conjugated SERS nanoprobes. Each of these platforms has its own characteristics and methods. Microfluidic chip platforms develop optofluidic immunoassay by accelerating of the binding between Ab and antigen and also minimizing the nonspecific binding of SERS nanoprobes. In case of SERS-based LFA platform, it involves lateral flow chromatographic diffusion and spectroscopic measurement of SERS nanoprobe by overcoming troubles of conventional naked eye detection LFA strips. Also, magnetic beads are generally used for achieving the separation and detection of target molecules more easily in the liquid phase. Chip-based platform is used as a fast and low-cost detection platform by consuming a little amounts of target molecules and probes. Due to these benefits, SERS-based immunoassay using sandwich complex platform have attracted magnificent attention for signal amplification ability.

On the other hand, various SERS-based immunoassay still has a lot of difficulties in applying it practical because most researchers only have focused on final results such as high sensitivity and limit of detection (LOD). In other words, there are few fundamental studies such as the optimization of primary Ab-affinity chip substrate, antigens and target Ab-affinity SERS nanoprobe. For instance, the number of antigens changing depending on the number of Abs conjugated on the nanoprobe have rarely been studied. Also, no study has been done to ensure that the capture Abs are densely immobilized on the substrate. This lack of study about fundamental immunoassay process makes it hard to get reliable and reproducible immunoassay results and this hardness prevent further development into a multiple detection platform.

To resolve these problems, we developed and validated a novel SERS-based immunoassay platform based on glass chip-immobilized substrate with our developed SERS nanoprobe. Chip-based immunoassay platform has advantages compared with other types of immunoassay platforms in terms of minimal sample consumption and low analyst concentrations[34] First, we synthesized and characterized three kinds of SERS Dots for showing multiplex capability of our immunoassay platform. Second, the Ab conjugation technique were optimized for evaluation of bioactivity

about SERS nanoprobe. In addition, we analyzed and compared immunoreactions between the Ab conjugated on the nanoprobe and the antigen in respect to the binding rate and coupling efficiency by utilizing fluorescence labeled Ab and antigen. Finally, the optimization of capture Ab onto the chip surface were implemented for the verification of the Ab surface density by utilizing fluorescence labeled Ab with high sensitivity.

Based on these validation experiments, we confirmed that our optimized SERS-based immunoassay platform can be used for detecting targeted biomarkers with high sensitivity. To verify our approach, we selected a prostate specific antigen (PSA) as a model biomarker which is used for diagnosing prostate cancer. Here, we present a SERS-based immunoassay platform using our validated chip substrate and SERS nanoprobes. All in all, we suggest that this immunoassay platform has a potential for the detection of various biomarkers due to its high sensitivity and multiplex detection capability.

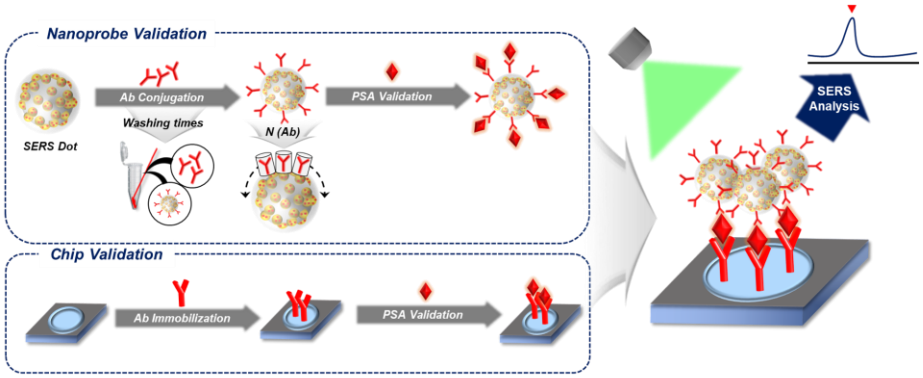

Scheme 1. Schematic illustration of optimized an immunoassay platform based on SERS nanoprobes. Based on nanoprobe validation and chip validation, sandwich immunocomplex is captured by chip substrate.

2. Experimental Section

2.1. Chemicals and Materials

Tetraethyl orthosilicate (TEOS), ammonium hydroxide (NH_4OH, 28-30%), 3-mercaptopropyltrimethoxysilane (MPTS), silver nitrate ($AgNO_3$, 99.99%), ethylene glycol, octylamine, sodium silicate, 4-fluorobenzenthiol (4-FBT), 4-bromobenzenthiol (4-BBT), 4-chlorobenzenthiol (4-CBT), 3-aminopropyltriethoxysilane (APTES), succinic anhydride, *N,N'*-diisopropylethylamine (DIEA), *N*-hydroxysuccinimide (NHS), dimethylaminopyridine (DMAP), *N,N'*-diisopropylcarbodiimide (DIC), Phosphate buffered saline (PBS, pH 7.4), bovine serum albumin (BSA, 98%), ethanolamine and Prostate Specific Antigen from human semen (PSA) were purchased from Sigma-Aldrich (St. Louis, MO, USA). Absolute ethanol (99.9%), anhydrous ethanol (99%) and *N*-methylpyrolidone (NMP) were purchased from Daejung Chemicals (Siheung, Korea). Alexa Fluor 532 labeled goat anti-mouse IgG (H+L) and Alexa Fluor 660 labeled goat anti-mouse IgG (H+L) were purchased from Invitrogen (Carlsbad, CA, USA). Alexa Fluor® 555 microscale protein labeling kit were purchased from Molecular Probes (USA). Epoxide-functionalized slide glasses were purchased from Array-it Corporation (Sunnyvale, CA, USA).

2.2. Synthesis of SERS Dots

SERS Dots were prepared as the previously reported method with slight modifications for this study.[35] Briefly, silica nanoparticles (SiNPs) with a diameter of *ca.* 170 nm were prepared by the Stöber method.[36] Next, silica surfaces were, functionalized with thiol groups by MPTS treatment and Ag domains (*ca.* 10 nm) were introduced on the surface of the thiol-functionalized silica sphere by the amine-assisted growth method.[37] Then, a 1-mL aliquot of 10-mM Raman label compound (RLC; 4-FBT, 4-BBT and 4-CBT, in ethanol) was added to 8 mg of the Ag-coated SiNPs. The resulting dispersion was shaken for 1 h at 25 ℃. The RLC-coded Ag-coated Si NPs were centrifuged and washed with ethanol twice. To encapsulate the Ag embedded SiNPs with a silica shell, the NPs were dispersed in 15 mL of dilute sodium silicate aqueous solution (0.036 *wt*% SiO2). The dispersion was stirred with a magnetic stirrer for 15 h at room temperature. Finally, 60 mL of ethanol, 250 μL of aqueous NH_4OH and 25 μL of TEOS were added to the reaction mixture, and stirred for 24 h at room temperature. The resulting SERS dots were centrifuged and washed with ethanol several times.

2.3. Bio-functionalization of SERS Nanoprobe

In order to bio-functionalize the SERS dots, the following steps of surface modification were proceeded. First, 1-mg of SERS dots were dispersed in 1-mL of 5 *v/v*% APTES solution in ethanol, and 10 μL of NH_4OH (27%) was added. The resulting mixture was shaken for 1 h at 50 ℃ and washed with ethanol several times, and then re-dispersed in 500 μL of NMP. Succinic anhydride (1.75 mg) was added to the APTES-treated SERS dot dispersion, followed by addition of 3.05 μL of DIPEA to introduce carboxyl group on the SERS dot. The resulting mixture was stirred for 2 h at room temperature. Subsequently, the carboxyl group-functionalized SERS dots were washed with NMP and then redispersed in 200-μL of anhydrous NMP. For activation of the carboxyl group, NHS (20 mg), DIC (27 μL), and DMAP (2.1 mg) were added to the dispersion. The resulting dispersion was stirred at room temperature for 1 h and then washed with NMP and PBS (pH 7.4).

A 25-μg of tracer Ab was added to the NHS-activated SERS dots dispersed in 200-μL of PBS. The mixture was incubated for 1 h at room temperature. The resulting dispersion was washed with PBS containing 0.1w/w% Tween 20 (TPBS), and redispersed in PBS after BSA (5w/w% in PBS) treatment. After removing the excess reagents by centrifugation

and washing, tracer Ab-conjugated SERS dots were dispersed in PBS and stored at 4 ℃ before use. For evaluation purpose of bio-functionality of SERS dots, fluorescence labeled PSA was used as follows. 5 μLof 1 mg/mL Ab conjugated SERS dot solutions (3×10^{11} particles/mL) were mixed with 45 μL of Alexafluor555-labeled-PSA solutions of various concentrations (0.01 – 200,000 ng/mL). Under mild shaking, the resulting dispersions were incubated for 3 h, and sequentially washed with TPBS several times. Finally, the SERS dots were re-dispersed in PBS (15 μL) before measurement. PSA-bound SERS dots dispersion was filled in a capillary tube and fluorescence signals were measured with a micro-Raman system (JY-Horiba, LabRam 300).

2.4. Preparation of Chip Surface

For fabrication of a capture substrate, the 96 spots arrayed sticker (Proteogen, Chuncheon, Korea) was attached on an epoxy-functionalized glass slide. The 1.5-μL aliquots of 100 μg/mL tracer Ab solutions were incubated on the arrayed spots of the substrate for 4 h in a humidity chamber at room temperature. Then, the slide was soaked in TPBS and PBS with shaking to remove unbound Abs from the substrates for 7 minutes.

2.5. Immunoassay Protocols for PSA Detection

As mentioned **2.4.**, tracer Ab is immobilized on chip surface. After then, the remaining non-reacted epoxy groups were blocked with ethanolamine (5 mM) in with PBS containing 3% (w/w) BSA for 30 min, and the unreacted reagents were washed with TPBS and PBS. The substrates were stored in PBS at 4 ℃ before use. In assay procedures, the capture substrate was exposed to the 1.5-μL aliquots of analytes (PSA) serially diluted with PBS containing 1% (w/w) BSA for 1 h in a humidity chamber. The three trials were replicates of each concentrations of 0.001 − 1000 ng/ml. After washing with TPBS and PBS, the antigen-captured substrate was exposed to 1.5 μL of the tracer Ab conjugated SERS dot dispersion for 2 h. Finally, the substrates, on which sandwich immunecomplexes were formed, were rinsed with TPBS, PBS and D.I. water, followed by drying gently.

2.6. Instrument and SERS Measurement

The size and morphology of the SERS Nanoprobes were characterized by using a TEM instrument (JEM1010, JEOL). The size and concentration of nanoparticles were determined by nanoparticle tracking analysis (NTA; Nanosight LM10, Malvern, Worcestershire, UK). The spot-arrayed slide was scanned with GenePixed or UV-vhologray Scanner (Axon Instruments, CA, USA) scanner using 532-nm laser-line for characterization of Ab immobilization and antigen-Ab interaction using Alexa Fluor 532 goat anti-mouse IgG (H+L) antibodies and Alexafluor555-labeled antigens. The scanner was set to optimize the quality of the microarray images by adjusting the laser power and contrast (Molecular Devices, CA, USA). For obtaining fluorescence spectrum and Raman spectrum, a conventional confocal microscope Raman system (LabRam 300, JY-Horiba, France) equipped with an optical microscope (BX41, Olympus, Japan) was utilized. In this Raman system, the Raman scattering signals were collected in a back-scattering geometry and detected by a spectrometer equipped with a thermo-electrically cooled CCD detector. The 532-nm line of a diode-pumped solid-state laser (Cobolt Samba^{TM}, Cobolt, Sweden) the 660-nm line of a diode-pumped solid state laser (Cobolt Samba^{TM}, Cobolt, Sweden) were used as an excitation source. For performing SERS-based

immunoassay, we used a Raman readout system for quantification of chip-based bioassays. The 532-nm excitation light (Compass 115M, Coherent Inc., USA) was delivered via a galvanometric mirror of the laser scanning unit to a sample through a 40× objective lens (NA 0.75, Olympus, Tokyo, Japan). The back-scattered light from the sample was collected by the same objective and filtered by a holographic notch filter to remove Rayleigh scattering lights. Then, the light signal was focused onto the entrance slit of the spectrometer (XPE200, NanoBase, Korea) in order to be detected with a thermoelectrically-cooled CCD (charge-coupled device, Princeton Instruments). In order to perform whole area scan while minimizing scanning time, single spectrum per frame is obtained without saving individual spectrum by keeping CCD camera open during single raster scan of whole area with high confocal geometry.

3. Results and Discussion

3.1. Characterization of SERS Dots

As illustrated in Figure 1-a), SERS Dots consist of Raman label compound (RLC)-coated silver domains embedded on a silica core (*ca.* 170 nm). Figure 1-b) and c) shows the TEM images of Ag-embedded SiNP and silica-coated SERS Dots. Ag domains and outer silica shells were well and homogeneously fabricated for applying further SERS-based immunoassay validation by observing TEM images. Next, to confirm the optical properties of SERS Dots, we measured NTA data and the intensity profile by nanoparticle tracking analysis (NTA) and micro-Raman. As shown in the graph of Figure 2, we confirmed that the size and dispersity data of three kinds of samples; each of them was well dispersed and has a narrow size distribution. It shows that SERS Dot have good stability and dispersity, which are efficiently applied for further surface modification. Figure 3-a) shows the SERS spectra of three kinds of different Raman chemical-labeled SERS Dots. The SERS $Dot_{4\text{-FBT}}$, SERS $Dot_{4\text{-BBT}}$ and SERS $Dot_{4\text{-CBT}}$ showed unique and distinguishable SERS bands (4-FBT: 386 cm^{-1}, 4-BBT: 488 cm^{-1}, 4-CBT: 541 cm^{-1}). Figure 3-b) shows SERS intensity distribution data for verifying signal homogeneity of each SERS Dot and marked lines in this

figure represent average signal intensity of each SERS Dots (4-FBT : 207.17, 4-BBT : 168.21, 4-CBT : 185.10) All 3 kinds of SERS Dots have efficient and uniform SERS signal for obtaining accurate assay data with SERS. This adequate and uniform intensities of SERS signals for SERS-based immunoassay are due to the ensemble averaged effect of AgNP which is assembled on silica surfaces. In addition, to verify the photostability of our SERS Dots, we measured three kinds of each single SERS Dot under laser irradiation (11.25 mW) for 300 s with 10 s time interval. (Figure 3-c)). The SERS intensity has not changed significantly with irradiated laser time in case of all kinds of SERS Dots, which means our synthesized SERS Dots have strong photostability. All of these results about SERS Dot characterization indicate that SERS Dots are sufficiently sensitive and uniform for single particle detection with little signal and size particle-to-particle variation and strong photostability for applying quantitative SERS-based immunoassay.

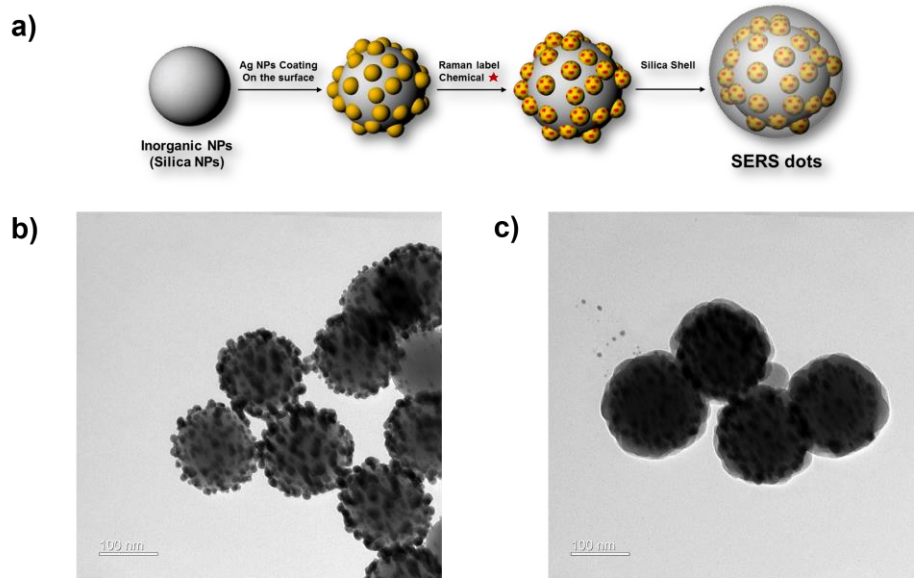

Figure 1. Schematic illustration of synthesis of SERS Dot. (a) Scheme of fabrication about SERS Dots. TEM images of (b) Ag-embedded silica and (c) SERS Dot.

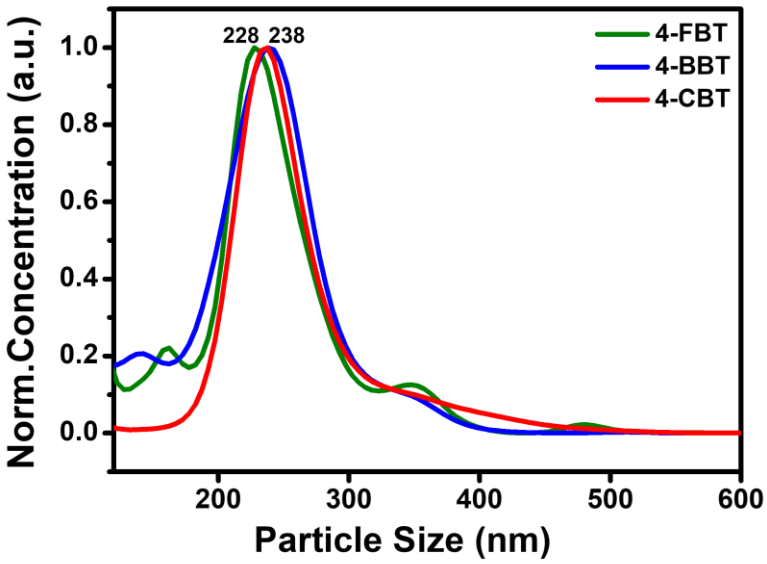

Figure 2. Size measurement and size distribution data with Nanoparticle Tracking Analysis (NTA). The plots represent particle size distribution of three kinds of different SERS Dots. The numbers written above the plots means the size of each SERS Dot (4-FBT, 4-BBT, 4-CBT).

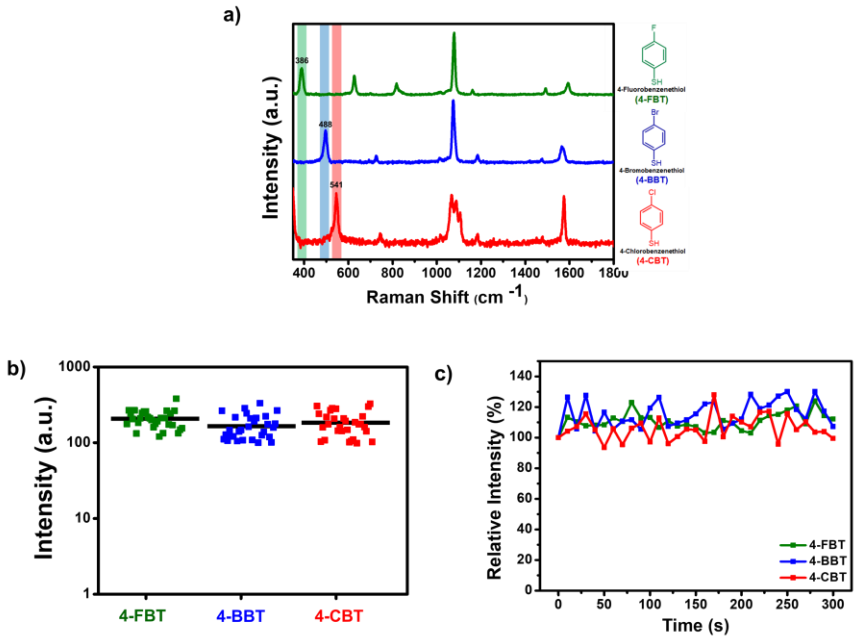

Figure 3. Characterization of SERS Dots with SERS signal. (a) Representative SERS spectra of 3 kinds of different SERS Dots. (b) SERS intensity distribution data for verifying signal homogeneity of each SERS Dots. (4-FBT: 386 cm-1, 4-BBT: 488 cm-1, 4-CBT: 541 cm-1) black line in data show the average intensities of each SERS Dots at their distinctive peak position (c) Photostability test data of a single SERS Dot. SERS intensity changes obtained from single SERS Dot with continuous laser exposure time (300s). All of spectra for characterization with SERS were obtained using micro-Raman system by the 532 nm photoexcitation of 11.25 mW at the sample and light acquisition time of 1s.

3.2. Evaluation of Bio-functionality about SERS Nanoprobes

Establishing and evaluating the fundamental technologies about SERS nanoprobes such as Ab conjugation technique and evaluation of bioactivity is essential process for successful immunoassay results. Especially, investigation of the number of antibodies introduced into the nanoparticles and their bioactivity has a great influence on the optimization of immunoassay platform validation. To verify and optimize our SERS nanoprobes, we performed some experiments related to Ab and SERS nanoprobes.

First, we optimized washing times during the Ab conjugation process onto SERS Dot surface. During the washing process, we observed that fluorescence intensity of SERS nanoprobes were changed irregularly in the step of conjugating fluorescence Ab on the surface of nanoparticles. Through the experiment, we observed unconjugated fluorescence Abs after 2 times washing which was followed by previous methods and this remained Abs were affected to find saturation point of fluorescence signal of nanoprobes. To solve this problem, the number of centrifuge times was increased to 8 times to remove unconjugated Abs in supernatant. After washing steps, fluorescence spectrum about the supernatant and the sample solutions (SiNP-AF532) were obtained and compared according to

washing time (Figure 3-a), b)). As illustrated in Figure 3-a), the intensity of the fluorescence decreased sequentially according to the number of centrifugation. In order to figure out more reliable number of washing times, fluorescence intensity profiles are converted to the y-axis log scale (Figure 3-b)). Through this result, the point where the supernatant fluorescence intensity and the solution fluorescence intensity (SiNP-AF532) were equal were found. It means that immobilized Ab is rarely presented which is not affected further immunoreaction in a liquid form. Based on this result, we found that in order to remove unconjugated Ab, the most optimized number of centrifugation is 4 times. For verifying our washing times, another experiment was conducted by changing the concentration of AF532 (10 – 80 μg). As in the process of Figure 4, the supernatant was extracted at each centrifugation step and then fluorescence intensity was measured. Figure 5 shows comparison about fluorescence intensity according to different AF532 concentration. It was confirmed that there was no big difference depending on concentration of AF532 which was same tendency in Figure 4. Through the analysis results of Figure 4-a) and b) and 5, we confirmed that most optimized number of centrifugation is 4 times in order to remove the unconjugated Ab on the surface of nanoparticle.

Next, after conjugating the fluorescence labeled Ab on the SiNP, based on the fluorescence signal, we counted the number of Abs which is immobilized on the surface of the nanoparticle. To calculate the number of Abs, we set up an Ab conjugation immobilization technique and carried out experiments to make standard methods. The Fluorescence labeled Ab (AF660) were conjugated on the surface of SERS Dot in order to experimentally and quantitatively evaluate the number of conjugated Abs on a single SERS Dot (Figure 6-a)). First, fluorescence intensity was measured with increasing the concentration of Ab (Figure 6-b)). According to this data, it was confirmed that the fluorescence intensity increased as the Ab concentration increased. Before the quantitative analysis, the concentration of SERS Dot was determined using NTA. As shown in Figure 6-a), each Ab conjugated SERS Dot was quantitatively analyzed based on the standard curve of the Ab (Figure 6-c)). A single SERS Dot with 230 nm diameter had *ca.* 44 antibodies on its surface. Theoretically, the surface area of a 230 nm sphere shaped nanoparticle corresponds to a covering area of *ca.* 900antibodies, assuming *ca.* a 15 nm diameter of each Ab.[38] To explain the calculation process about conjugated Abs onto nanoparticle surfaces, we proposed Ab calculation method based on some parameters. Figure 6-d) shows the calculation

formula about our Ab calculation method. For example, the fluorescence intensity of concentration 250 μg AF660 is 5436.07 at fluorescence intensity profile of Figure 6-b). Substituting 5436.07 for the value of y in the calibration curve (y=30723.58x-14700) of Figure 6-c), the actual concentration of Ab (Conc.of Ab) obtained through calibration curve is 0.66 μg/mL. The molecular weight of the Ab (Mass of Ab) was converted by the molecular mass of IgG Ab to 150 kDa. As illustrated in Figure 6-d)-Eq 1, total amount Ab to nanoparticle surface is 5.3×10^{11} (Conc.of Ab: 0.66 μg/mL, Mass of Ab: 2.65×10^{12}, Volume: 0.20 mL). Finally, total amount Ab to nanoparticle surface was divided into the total number of SERS Dot (1.20×10^{11} by NTA) and indirectly confirmed that about 44 antibodies were immobilized per SERS Dot nanoparticle. By calculating presented Figure 6-d)-Eq 1 and 2, the number of immobilized antibodies per SERS Dot was quantified in Figure 6-b). As the intensity of fluorescence increased, the number of immobilized Abs per SERS Dot was also increased. Through this result, this is proved that optimized Ab immobilized technique was well established for applying SERS-based immunoassay platform.

In another aspect, it is essential to evaluate bio-functionality of nanoprobes for efficiently applying to immunoassay platform. So, we

confirmed bio-functionality of our SERS nanoprobes by reacting and measuring fluorescence-labeled PSA antigen with PSA tracer Abs which is conjugated on SERS nanoprobes. In this experiment, bio-functionality of the SERS nanoprobes was verified using Alexafluor555-labeled PSA (AF555-PSA). As illustrated in Figure 7-a), we prepared PSA-tracer Ab conjugated SERS dot (PSA-SERS nanoprobes, Experimental group) which is capable of specifically binding to PSA, and IgG Ab conjugated SERS dot (IgG-SERS nanoprobes, Control group) which is not specifically bound to PSA. After then, each SERS nanoprobes was incubated with various concentrations of AF555-PSA solutions (0.1 – 200,000 ng/mL) and washed out to remove unbound antigens. Figure 7-b) shows the fluorescence spectra of the PSA-SERS nanoprobes and Figure 7-c) shows the fluorescence spectra of the IgG-SERS nanoprobes with conjugating AF555-PSA. The fluorescence intensity of AF555-PSA treated PSA-SERS nanoprobe solutions increased with increase of AF555-PSA concentrations, while the IgG-SERS nanoprobe showed negligible increase of the signal intensity. To evaluate the antigen binding capacity of PSA-SERS dots, the number of bound AF555-PSA was estimated using the standard curve ($y=145.98x$) obtained from fluorescence

signal intensities of free AF555-PSA. For the case of SERS dots with the highest fluorescence intensity, the Ab concentration was estimated to 239 ng/ml from the standard curve. That means that the final solution (15 μL) contained 1.4×10^9 PSA molecules bound to SERS dots, and the number of PSA molecules captured on a single Ab-conjugated SERS dot was 45 in average. As a result, it was found that more than half of the PSA-tracer Ab specifically bound PSA and this result verified that theour fabricated SERS nanoprobe has good bio-functionality.

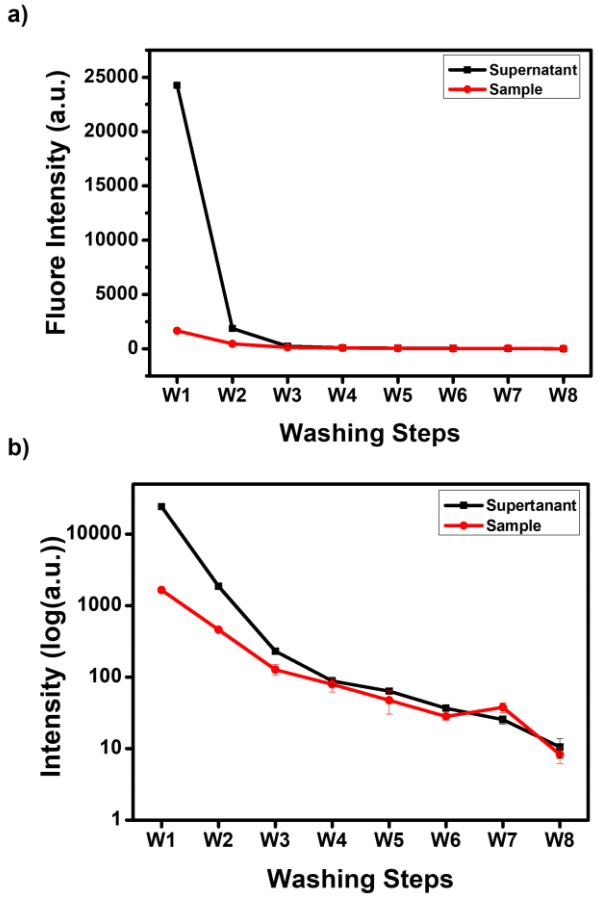

Figure 4. Optimization of washing times after antibody incubation using SiNP. (a) Fluorescence intensity profile for the Comparison of the fluorescence intensities about supernatant and sample solutions (SiNP – AF532) according to number of washing times. (b) Fluorescence intensity profile with changing y-axis of graph (a) to log scale. Fluorescence profiles were obtained using micro-Raman system with the 532 nm photoexcitation of 0.053 mW.

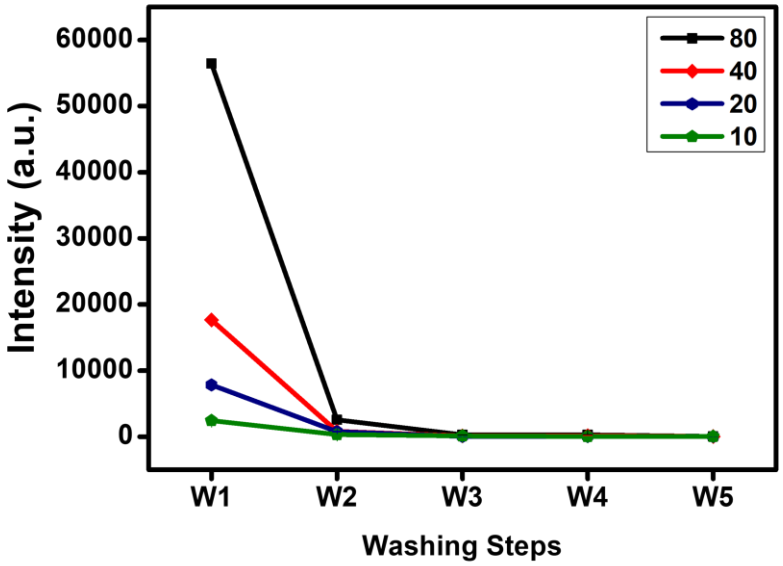

Figure 5. Fluorescence intensity profiles of supernatant solution after washing. Supernatant is measured by washing time with controlling AF532 concentration (10 – 80 μg) using 1 mg SiNP. Fluorescence profiles were obtained using micro-Raman system with the 532 nm photoexcitation of 0.053 mW.

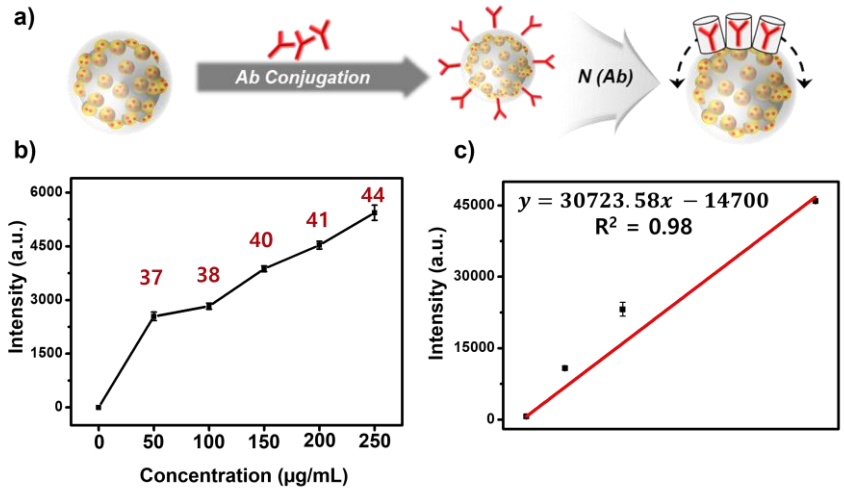

d)

Eq 1. $\frac{Conc.of\ Ab\ (calculated\ from\ graph\ (c))}{Mass\ of\ Ab}$ X Volume

= *Total Amount Ab to nanoparticle surface*

Eq 2. $\frac{Total\ Amount\ of\ Ab\ to\ nanoparticle\ Surface}{total\ nanoparicle}$ = Ab / NP

Figure 6. Validation of antibody immobilization and counting the amounts of antibodies on SERS Dot surfaces. (a) Schematic illustration of incubated fluorescent labeled antibody (AF660) immobilized into nanoparticle. (b) Fluorescence intensity profile as incubated with changing AF660 concentration. (c) Standard curve of AF660 with fluorescence intensity of reference AF660 sample. (d) Summary of calculation process about counting antibodies on a single nanoparticle surface. Calculation results are marked on graph (b) according to concentration of AF660.

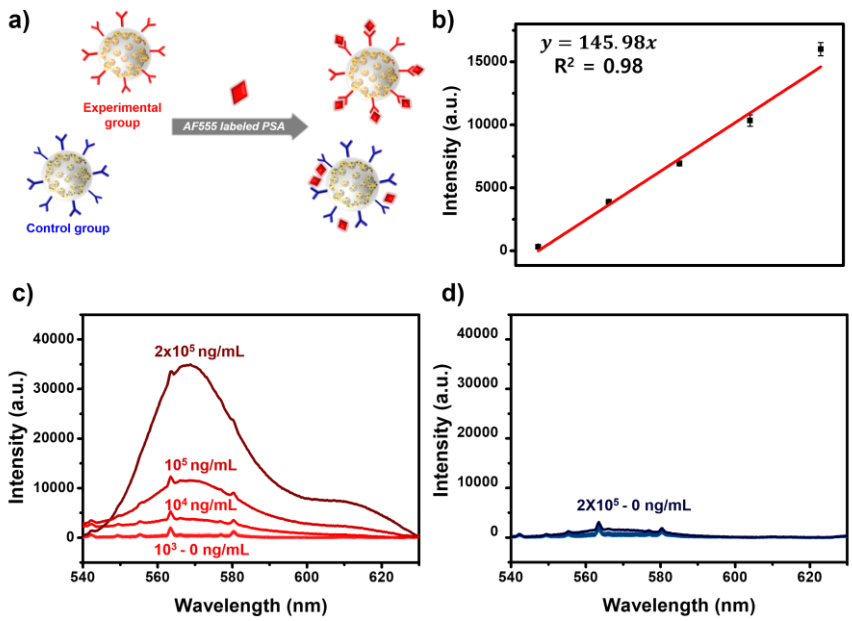

Figure 7. Validation of biocompatibility about SERS nanoprobes. (a) Schematic illustration for biocompatibility validation and optimization. (b) Standard curve of AF555 labeled PSA with fluorescence intensity of reference AF555 labeled PSA sample. Comparison in the (c) experimental group and (d) control group for measuring each fluorescence intensity.

3.3. Optimization of Capture Antibody onto Chip Surface

For evaluating sensitive immunoassay platform, optimization of capture Ab onto chip surface is crucial issue because of its importance in terms of sandwich immunoreaction system with SERS nanoprobes and antigens which is related directly into sensitivity and reproducibility of immunoassay platform.

First, optimization of Ab immobilization step was needed for fabricating capture substrate (Figure 8-a)), because Ab surface density is important about detection sensitivity. Increased surface density of capture Ab generally offers improved capturing capacity of target antigen. To determine the conditions about fully-covered Ab onto chip surface, fluorescence signal based analysis was carried out using AF532. An epoxy-functionalized slide glass was incubated with the various concentrations of AF532 solutions (10 – 1000 μg/mL) immobilized for 4 h. After immobilization, we measured fluorescence of AF532 onto chip surfaces by microarray scanner (Figure 8-b)). Fluorescence scanning image shows that the higher concentration of immobilizing AF532 led to higher density of capture Ab immobilization (Figure 8-b)) and signal saturation was observed 100 – 1000 μg/mL. However, considering the fluorescence intensity profile (Figure 8-c)) and the possibility of

remaining unfixed Ab on chip surface at high concentration, the concentration of Ab to be fixed on the chip is set at 100 μg/mL. However, considering the fluorescence intensity profile (Figure 8-c)) and further signal increase were not observed. As a result, we set the concentration of capture Ab as 100 μg/mL for immobilizing chip surface. Then, when Ab was immobilized on the chip surface, it was confirmed that the Ab concentration of 100 μg/mL was saturated on the surface at the same time.

Another factor for optimizing chip surface immobilization is conjugation time. We incubated epoxy-functionalized slide glass with AF532 solutions (50, 100 μg/mL) at the different times (2 – 24 h) to determine the optimized time for fully-covering capture Ab onto chip surfaces. As shown in Figure 8-d), in case of saturated time below 2 h, fluorescence intensity is much lower than other incubated times. In case of saturated time over 8h, fluorescence intensity was gradually saturated. Incubation time among the 4 h and 8 h, for in further assay experiment, 4 h is the most optimized time on the basis about immobilization time of antigen and nanoprobes, fluorescence intensity and their standard deviation. Through these results, we found optimized immobilization condition, such as the 4 h for incubation time and the 100 μg/mL for Ab concentration, to guarantee high density of capture Ab.

Second, verifying bio-activity of target antigen (PSA) onto immobilized chip surfaces was important for sandwich type immunoassay platform. For that reason, we performed bio-functionality of chip surface using AF555-PSA. As illustrated in Figure 9-a), after immobilizing the Ab (experiment group: PSA-capture Ab, control group: IgG Ab and PBS solution) on the surface of the chip, we confirmed that whether the immobilized Ab is specifically bound to the antigen or not. AF555-PSA with concentrations of $10 - 10^5$ ng/mL were used to confirm the on-chip antigen binding. Comparing the fluorescence graphs of the experimental group (PSA-capture Ab) in which concentration of $10 - 10^5$ ng/mL of PSA antigen were immobilized and control group (IgG, PBS), it was confirmed that PSA-capture Ab well conjugated with high specificity (Figure 9-b)). Through these results, we verified that bioactivity about PSA-capture Ab binds specifically to the target antigen (PSA).

At the end, it is essential to confirm that non-specific binding of SERS nanoprobes for lowering measurement errors when SERS-based immunoassay performed. So, we performed several experiment for optimizing chip surfaces. We confirmed and optimized conditions about preventing non-specific binding of SERS nanoprobes onto chip surfaces. This process is essential step for evaluating sensitivity and accuracy of our

immunoassay platform. As illustrated in Figure 10-a), after capture-Ab is immobilized on the epoxy-functionalized slide glass, the unreacted epoxy functional groups remaining on the slide glass were blocked with 5 mM of ethanolamine in BSA (3*w/w* %) or BSA (1*w/w* %) and then unreacted reagents are washed alternately with TPBS and PBS. The reason for using BSA in the blocking process is to minimize the non-specific binding of SERS nanoprobes and evaluate biocompatibility of target antigen. Finally, SERS nanoprobes were raised up to the blocking slide glass. All of this process is due to determine whether the epoxy functional groups are well blocked or not and also to find the optimal ratio of concentration for blocking. The results of the experimental group (Figure 10-b)), BSA (3*w/w* %)) and control group (Figure 10-c), BSA (1*w/w* %)) shows that to minimize non-specific binding of SERS nanoprobes. In the experimental group (Figure 10-b)), it was confirmed that no SERS nanoporbes were observed by the confocal microscope image. On the other hand, in the case of the control group (Figure 10-c)), SERS nanoprobes were observed in the optical image using the confocal microscope. Overall, nonspecific binding did not occur during immunoassay and optimized blocking solution condition have 3*w/w* % BSA for effective reducing of nonspecific binding.

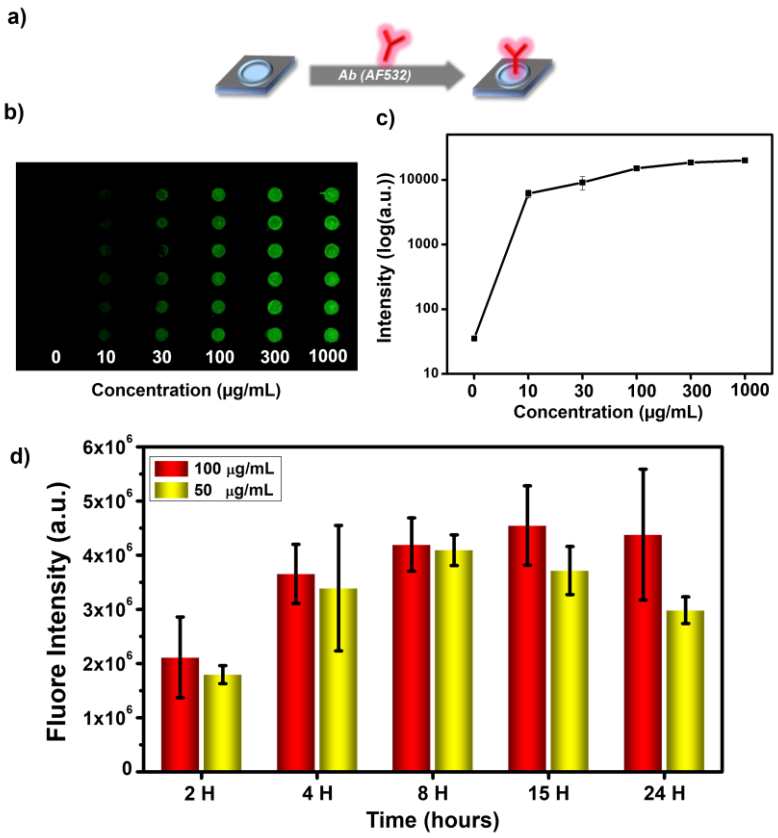

Figure 8. Optimization of capture Ab immobilization onto chip surface. (a) Schematic illustration of immobilization of capture antibody onto chip surface. (b) Fluorescence scanning image of spot-arrayed slide with different AF532 concentration. (c) Fluorescence intensity profiles of immobilized antibodies with different AF532 concentration. (d) Fluorescence intensity of immobilized AF532 onto chip surfaces with different immobilization time (red bar: 100 μg/mL, yellow bar: 50 μg/mL).

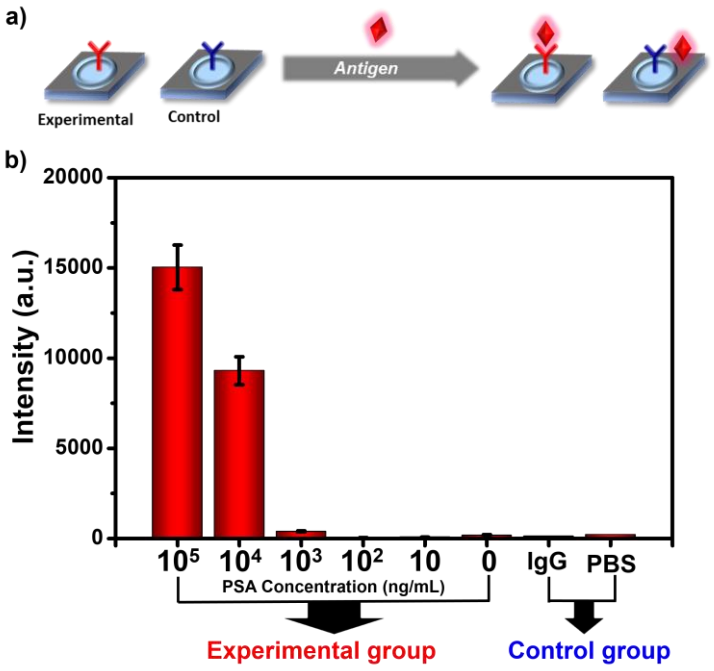

Figure 9. Verification of bioactivity about target antigen (PSA) onto immobilized chip surfaces. (a) Schematic illustration of conjugating PSA on the PSA capture Ab immobilized surfaces. (b) Fluorescence intensity profiles with various Alexa-fluor 555 labeled PSA concentration (0 – 105 ng/mL) and control groups (IgG and PBS).

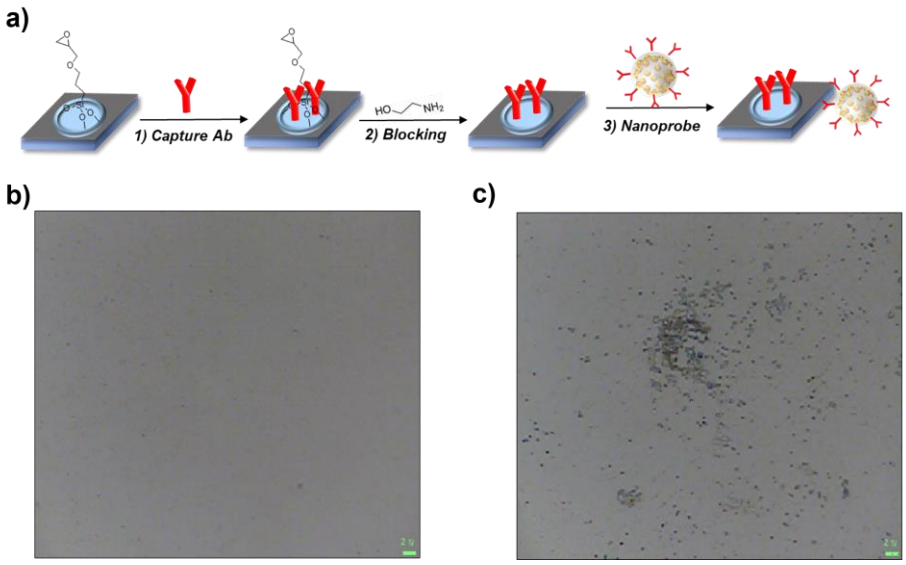

Figure 10. Experimental data for preventing non-specific binding of SERS nanoprobes. Optical images of samples on (a) experimental group and (b) control group

3.4. PSA Detection with SERS-based Immunoassay

PSA, which is used for biomarker of prostate cancer diagnosis, was selected for validation of the immunoassay platform. PSA at 0.0001 − 1 ng/mL was incubated on the capture substrate, followed by incubation with SERS nanoprobe (tracer Ab - conjugated SERS Dot) to enable selective targeting of captured PSAs. After forming sandwich complexes, SERS intensities were measured using Raman readout system. The SERS spectra from each sample were measured by scanning the areas of 200 × 200 μm, followed by averaging of three spots. As shown in Figure 11-a), unique bands of SERS $Dots_{4\text{-FBT}}$ (386, 623, 814 and 1075 cm^{-1}) were evident, the intensities of which increased with increasing PSA concentration. A standard calibration curve was obtained by plotting the intensity of 1075 cm^{-1} band as a function of the logarithm of PSA concentration (Figure 11-b)), exhibiting a wide dynamic range of detection from 0.0001 to1 ng/mL. The plot exhibited strong linearity (R^2 = 0.99) over five orders of magnitude below 10 ng/mL PSA. This assay platform that yields consistent results at low and high concentrations is useful in terms of integration of tools for diagnosis and monitoring of disease status. The limit of detection (LOD), defined as the analyte

concentration that produces a signal three-fold higher than the standard deviation of blank measurements (2164 in this experiment), was 0.05 pg/mL. This suggests a wider dynamic range with lower LOD compared to a recently reported enzyme-linked immunosorbent assay for PSA.

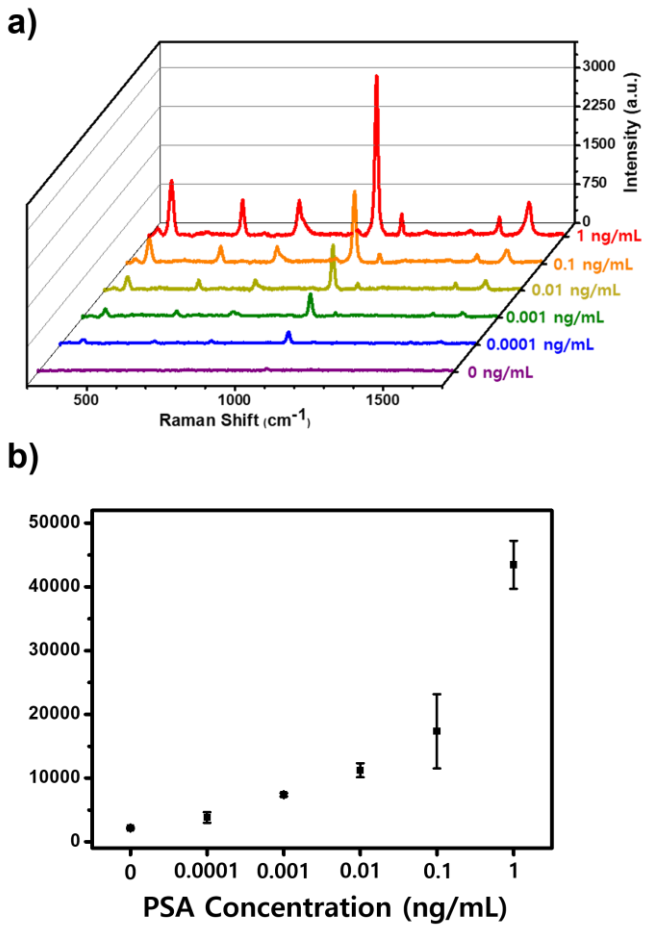

Figure 11. Schematic illustration of a chip-based immunoassay using SERS Dots and an area-scanning readout system. (a) Raman spectra from sample of PSA various concentration (0.0001 – 1 ng/mL). Representative samples each concentration. (b) Correlation plots between the area densities of SERS dots and the relative Raman intensity at 1075 cm-1 band of 4-FBT.

4. Conclusion

In summary, we demonstrated a validation and optimization of SERS-based immunoassay platform using our developed SERS nanoprobes and a chip substrate for getting reproducible and reliable results. First of all, we showed uniformity and stability of SERS Dots which are sufficiently detectable and photostable at the single probe level. Next, the number of Abs on the nanoprobe and captured antigens were evaluated by utilizing fluorescence-labeled Ab and antigen. It reveals that specificity were confirmed by calculating the number of Ab and captured antigen using fluorescence signal. In addition, chip substrate was optimized successfully by controlling the incubation conditions (incubation time: 4 H, incubation concentration: 100 μg/mL) using fluorescence labeled Ab. Likewise, SERS nanoprobe evaluation test, we ensured that specificity and validation was well performed using Ab which is immobilized on chip substrate and fluorescence labeled antigens. Finally, for the preventing nonspecific binding, we indicated blocking solution condition with 3*w/w* % BSA with 5 mM of ethanolamine for effective reducing of nonspecific binding.

In the last part of experiment, we applied this validated SERS-based immunoassay platform to real biomarker detection. We chose PSA as

model biomarker, the limit of detection of the PSA biomarker was found to be (ca. 0.05 pg/mL LOD) with a wide dynamic range (0.0001 – 1 ng/mL). Thus, we confirmed that our optimized SERS-based immunoassay platform has an extended potential for diagnosis of other diseases including prostate cancer and multiplex capacity.

5. References

1. Farka, Z., Jurik, T., Kovar, D., Trnkova, L. & Skladal, P. Nanoparticle-Based Immunochemical Biosensors and Assays: Recent Advances and Challenges. *Chem Rev* **117**, 9973-10042 (2017).

2. Wang, Z., Zong, S., Wu, L., Zhu, D. & Cui, Y. SERS-Activated Platforms for Immunoassay: Probes, Encoding Methods, and Applications. *Chem Rev* **117**, 7910-7963 (2017).

3. Fu, X., Chen, L. & Choo, J. Optical Nanoprobes for Ultrasensitive Immunoassay. *Anal Chem* **89**, 124-137 (2017).

4. Chao, J. et al. Nanostructure-based surface-enhanced Raman scattering biosensors for nucleic acids and proteins. *Journal of Materials Chemistry B* **4**, 1757-1769 (2016).

5. Harper, M.M., McKeating, K.S. & Faulds, K. Recent developments and future directions in SERS for bioanalysis. *Phys Chem Chem Phys* **15**, 5312-5328 (2013).

6. Borrebaeck, C.A.K. Antibodies in diagnostics – from immunoassays to protein chips. *IMMUNOLOGY TODAY* **21**, 379-382 (2000).

7. Lang, Q. et al. Specific probe selection from landscape phage display library and its application in enzyme-linked immunosorbent assay of free prostate-specific antigen. *Anal Chem* **86**, 2767-2774 (2014).

8. Xuan, Z. et al. Plasmonic ELISA based on the controlled

growth of silver nanoparticles. *Nanoscale* **8**, 17271-17277 (2016).

9. Jia, C.P. et al. Nano-ELISA for highly sensitive protein detection. *Biosens Bioelectron* **24**, 2836-2841 (2009).

10. Kim, C., Hoffmann, G. & Searson, P.C. Integrated Magnetic Bead-Quantum Dot Immunoassay for Malaria Detection. *ACS Sens* **2**, 766-772 (2017).

11. Speranskaya, E.S. et al. Polymer-coated fluorescent CdSe-based quantum dots for application in immunoassay. *Biosens Bioelectron* **53**, 225-231 (2014).

12. Law, W.-C., Yong, K.-T., Baev, A. & Prasad, P.N. Sensitivity Improved Surface Plasmon Resonance Biosensor for Cancer Biomarker Detection Based on Plasmonic Enhancement. *ACS Nano* **5**, 4858-4864 (2011).

13. Vashist, S.K., Schneider, E.M. & Luong, J.H. Surface plasmon resonance-based immunoassay for human C-reactive protein. *Analyst* **140**, 4445-4452 (2015).

14. Zhao, L., Wang, D., Shi, G. & Lin, L. Dual-labeled chemiluminescence enzyme immunoassay for simultaneous measurement of total prostate specific antigen (TPSA) and free prostate specific antigen (FPSA). *Luminescence* (2017).

15. Cho, I.H., Paek, E.H., Kim, Y.K., Kim, J.H. & Paek, S.H. Chemiluminometric enzyme-linked immunosorbent assays (ELISA)-on-a-chip biosensor based on cross-flow chromatography. *Anal Chim Acta* **632**, 247-255 (2009).

16. Sanchez-Purra, M. et al. Surface-Enhanced Raman Spectroscopy-Based Sandwich Immunoassays for Multiplexed Detection of Zika and Dengue Viral Biomarkers. *ACS Infect Dis* **3**, 767-776 (2017).

17. Le, T.T. et al. Dual Recognition Element Lateral Flow Assay Toward Multiplex Strain Specific Influenza Virus Detection. *Anal Chem* **89**, 6781-6786 (2017).

18. Tang, B. et al. Ultrasensitive, Multiplex Raman Frequency Shift Immunoassay of Liver Cancer Biomarkers in Physiological Media. *ACS Nano* **10**, 871-879 (2016).

19. 0.Cheng, Z. et al. Simultaneous Detection of Dual Prostate Specific Antigens Using Surface-Enhanced Raman Scattering-Based Immunoassay for Accurate Diagnosis of Prostate Cancer. *ACS Nano* **11**, 4926-4933 (2017).

20. Schlucker, S. Surface-enhanced Raman spectroscopy: concepts and chemical applications. *Angew Chem Int Ed Engl* **53**, 4756-4795 (2014).

21. Stiles, P.L., Dieringer, J.A., Shah, N.C. & Van Duyne, R.P. Surface-enhanced Raman spectroscopy. *Annu Rev Anal Chem (Palo Alto Calif)* **1**, 601-626 (2008).

22. Chang, H. et al. PSA Detection with Femtomolar Sensitivity and a Broad Dynamic Range Using SERS Nanoprobes and an Area-Scanning Method. *ACS Sensors* **1**, 645-649 (2016).

23. OKADA, H., HOSOKAWA, K. & MAEDA, M. Power-Free Microchip Immunoassay of PSA in Human Serum for Poing-of-

Care Testing. *ANALYTICAL SCIENCES* **27** (2011).

24. Li, J.-M. et al. Multiplexed SERS detection of DNA targets in a sandwich-hybridization assay using SERS-encoded core–shell nanospheres. *Journal of Materials Chemistry* **22** (2012).

25. Barbosa, A.I., Gehlot, P., Sidapra, K., Edwards, A.D. & Reis, N.M. Portable smartphone quantitation of prostate specific antigen (PSA) in a fluoropolymer microfluidic device. *Biosens Bioelectron* **70**, 5-14 (2015).

26. Kaminska, A. et al. Detection of Hepatitis B virus antigen from human blood: SERS immunoassay in a microfluidic system. *Biosens Bioelectron* **66**, 461-467 (2015).

27. Lee, M., Lee, K., Kim, K.H., Oh, K.W. & Choo, J. SERS-based immunoassay using a gold array-embedded gradient microfluidic chip. *Lab Chip* **12**, 3720-3727 (2012).

28. Wang, X. et al. Simultaneous Detection of Dual Nucleic Acids Using a SERS-Based Lateral Flow Assay Biosensor. *Anal Chem* **89**, 1163-1169 (2017).

29. Banerjee, R. & Jaiswal, A. Recent advances in nanoparticle-based lateral flow immunoassay as a point-of-care diagnostic tool for infectious agents and diseases. *Analyst* (2018).

30. Choi, S. et al. Quantitative analysis of thyroid-stimulating hormone (TSH) using SERS-based lateral flow immunoassay. *Sensors and Actuators B: Chemical* **240**, 358-364 (2017).

31. Wang, R. et al. Highly Sensitive Detection of Hormone Estradiol E2 Using Surface-Enhanced Raman Scattering Based

Immunoassays for the Clinical Diagnosis of Precocious Puberty. *ACS Appl Mater Interfaces* **8**, 10665-10672 (2016).

32. Yang, K., Hu, Y. & Dong, N. A novel biosensor based on competitive SERS immunoassay and magnetic separation for accurate and sensitive detection of chloramphenicol. *Biosens Bioelectron* **80**, 373-377 (2016).

33. Yu, J. et al. SERS-based genetic assay for amplification-free detection of prostate cancer specific PCA3 mimic DNA. *Sensors and Actuators B: Chemical* **251**, 302-309 (2017).

34. Gao, R., Cheng, Z., deMello, A.J. & Choo, J. Wash-free magnetic immunoassay of the PSA cancer marker using SERS and droplet microfluidics. *Lab Chip* **16**, 1022-1029 (2016).

35. Kim, J.H. et al. Encoding peptide sequences with surface-enhanced Raman spectroscopic nanoparticles. *Chem Commun (Camb)* **47**, 2306-2308 (2011).

36. Stöber, W. & Fink, A.B., E. Controlled Growth of Monodispersed Silica Sphere in the Micron Size Range. *J. Colloid Interface Sci.* **26**, 62-69 (1968).

37. Kang, H. et al. Base Effects on Fabrication of Silver Nanoparticles Embedded Silica Nanocomposite for Surface-Enhanced Raman Scattering (SERS). *Journal of Nanoscience and Nanotechnology* **11**, 579-583 (2011).

38. Jeong, S. et al. Highly robust and optimized conjugation of antibodies to nanoparticles using quantitatively validated protocols. *Nanoscale* **9**, 2548-2555 (2017).

국문 초록

최근 좁은 선폭과 높은 민감도의 장점을 지닌 표면 증강 라만 산란 (Surface-enhanced Raman Scattering, SERS) 기반의 면역 분석법은 생체 마커들을 특이적으로 검출할 수 있는 진단 기술로서 많은 관심과 연구가 이루어지고 있다. 하지만, 면역진단법을 수행하는 각 단계에서의 유효성 검증 및 최적화에 관한 연구가 부족한 상황이고, 이로 인해 SERS 기반의 면역진단기술을 실용화하는데 많은 연구자들이 어려움을 겪고 있는 상황이다.

이러한 문제점을 해결하기 위해, 본 연구에서는 SERS 기반 면역 분석 플랫폼의 유효성 검증 및 최적화 과정을 통해서 보다 더 재현성 있고 신뢰성 있는 칩 기반의 면역분석 플랫폼을 구현하기 위한 실험을 진행하였다. 면역 분석 진단기법 이를 위해 (1) 서로 다른 3 종의 신호를 내는 SERS Dot 을 합성하고 단일 입자 수준의 SERS 신호 검출을 통해 각각의 신호의 균일성과 안전성을 검증하였다. (2) 나노프로브의 유효성 검증: 항체 고정 기술을 최적화하고, 이를 바탕으로 항원과의 결합을 통해 생체활성도를 확인하였다. (3) 칩 플랫폼의 유효성 검증: 포획 항체를 기판 위에 고정시키는 실험 과정을 최적화하였고, 이를 바탕으로 칩 플랫폼의 생체활성도를 확인하였으며 비특이적 결합을 통제할 수 있는 조건을 찾기 위한 실험을 진행하였다. 위의 유효성 검증 및 최적화 실험에서 얻은 결과물을 바탕으로 확립된 SERS 기반 면역 진단기술 플랫폼의 유효성을 검증하기 위해 전립선암 특이항원 (PSA)을 0.05 pg/mL 수준으로 검출하는 데 성공하였고,

5 자리수의 넓은 검출 범위를 갖는 것으로 평가되었다. 본 연구의 결과를 바탕으로 SERS 기반의 면역분석 플랫폼에 있어 재현성과 유효성을 높일 수 있을 것으로 보이며 더 나아가 다양한 종류의 질병들을 효율적으로 검출 및 진단할 수 있는 플랫폼 개발에도 도움이 될 것으로 예상된다.

주요어: 표면 증강 라만 산란 (SERS), 면역 분석법, 샌드위치 면역복합체 플랫폼, 유효성 검증, SERS 나노프로브, 전립선암 특이항원 (PSA), 고감도 검출

학번: 2016-21587